

Hydrothermal synthesis of lindgrenite with a hollow and prickly sphere-like architecture

Jiasheng Xu, Dongfeng Xue*

State Key Laboratory of Fine Chemicals, Department of Materials Science and Chemical Engineering, School of Chemical Engineering, Dalian University of Technology, 158 Zhongshan Road, Dalian 116012, PR China

Received 4 April 2006; received in revised form 12 September 2006; accepted 25 September 2006
Available online 10 October 2006

Abstract

Lindgrenite $[\text{Cu}_3(\text{OH})_2(\text{MoO}_4)_2]$ with a hollow and prickly sphere-like architecture has been synthesized via a simple and mild hydrothermal route in the absence of any external inorganic additives or organic structure-directing templates. The hierarchical lindgrenite particles are hollow and prickly spheres, which are comprised of numerous small crystal strips that are aligned perpendicularly to the spherical surface. Two factors are important for the formation of hollow and prickly architecture in the present process. One is the general phenomenon of Ostwald ripening in solution, which can be responsible for the hollow structure; the other is that lindgrenite crystals have a rhombic growth habit, which plays an important role in the formation of prickly surface. Furthermore, $\text{Cu}_3\text{Mo}_2\text{O}_9$ with the similar size and morphology can be easily obtained by a simple thermal treatment of the as-prepared lindgrenite in air atmosphere.

© 2006 Elsevier Inc. All rights reserved.

Keywords: Lindgrenite; $\text{Cu}_3\text{Mo}_2\text{O}_9$; Hollow sphere; Prickly sphere; Hydrothermal synthesis

1. Introduction

The chemical synthesis of inorganic materials with unusual and novel architectures has attracted considerable attention, due to the fact that the shape and texture of materials strongly influence their properties [1–4]. Synthesizing inorganic materials with complex architectures could therefore be relevant to the design of new type inorganic materials. In particular, the hollow sphere with a nanometer to micrometer scale is one of important forms among various morphologies, which has some promising applications such as controlled-release capsules of various substances (drugs, cosmetics, and dyes), photonic crystals, catalysts, sensors, and chemical reactors [5–11]. The general approach for preparing such hollow structures is based on the use of various templates [5–11]. Nevertheless, the introduction of templates or other additives into the synthetic route undoubtedly leads to more synthetic

procedures and causes impurities in the final products. Therefore, developing simple template-free methods seems to be more promising due to various expected advantages, such as the relatively low cost, high purity, and large-scale production.

Molybdenum oxide-based materials are of contemporary interest due to their promising applications in the area of catalysis, absorption, electrical conductivity, magnetism, photochemistry, sensors, and energy storage [12–21]. Copper-based compounds are also the most important materials, which have been widely used in the area of catalysis, ion exchange, proton conductivity, intercalation chemistry, photochemistry, and chemistry materials [22,23]. For example, atacamite $[\text{Cu}_2(\text{OH})_3\text{Cl}]$, malachite $[\text{Cu}_2(\text{OH})_2\text{CO}_3]$, and libethenite $[\text{Cu}_2(\text{OH})\text{PO}_4]$ have been widely investigated due to their special properties and applications [24–27]. As one of comparatively rare copper minerals, lindgrenite $[\text{Cu}_3(\text{OH})_2(\text{MoO}_4)_2]$ was originally found in Chile and first described by Palache [28]. Recently, lindgrenite has attracted extensive interests in various research fields [29–32], for example, its crystal

*Corresponding author. Fax: +86 411 8899 3623.

E-mail address: dfxue@chem.dlut.edu.cn (D. Xue).

structure, Raman spectra, catalytic effect, and thermal decomposition behavior (from lindgrenite to $\text{Cu}_3\text{Mo}_2\text{O}_9$) have been widely investigated.

It is well accepted that there is a close relationship between the morphology and their properties of inorganic materials, i.e., the morphology influences their properties since the crystal shape dictates the interfacial atomic arrangement of materials. However, the reports on the growth and morphology of lindgrenite crystals are very few. Herein, we report a simple hydrothermal route (in the absence of any inorganic additives or organic templates) to synthesize lindgrenite with a hierarchical sphere-like architecture. To the best of our knowledge, such a hollow and prickly sphere-like architecture of lindgrenite has not been reported.

2. Experimental section

The lindgrenite microspheres were synthesized by hydrothermal treatment of a $\text{Cu}(\text{CH}_3\text{COO})_2$ (hereafter abbreviated as CuAc_2) solution in the presence of Na_2MoO_4 at 110°C . The starting solutions of analytical grade CuAc_2 and Na_2MoO_4 were freshly prepared. Synthetic lindgrenite microspheres were prepared by the titration of a 0.25 M CuAc_2 solution with a 0.25 M Na_2MoO_4 solution under vigorous stirring at room temperature for 30 min, then ultrasonicated for 10 min. The bluish slurry mixture was transferred into a Teflon-lined stainless steel autoclave of 80 mL capacity, filled up to 70% of the total volume. The autoclave was sealed and heated at $50\text{--}110^\circ\text{C}$ for 1–12 h in an electric oven, the autoclave was then cooled down to room temperature naturally. Green precipitates were filtered and washed with deionized water and anhydrous ethanol (respectively), several times; the final products were dried at 50°C (more than 5 h) for further characterizations. The phase and crystallographic structure of the samples were determined by powder X-ray diffraction (XRD, D/Max 2400, Rigaku, by a diffractometer equipped with the graphite monochromatized $\text{CuK}\alpha$ radiation) in the 2θ angles ranging from 10° to 70° . The morphology and size of these microspheres were characterized by scanning electron microscope (SEM, JSM-5600LV, JEOL). FT-IR spectra were recorded on a Fourier transform infrared spectrometry (FT-IR, KBr disc method; NEXUS) in the range of $400\text{--}4000\text{ cm}^{-1}$.

3. Results and discussion

Lindgrenite [$\text{Cu}_3(\text{OH})_2(\text{MoO}_4)_2$] crystallizes in a monoclinic space ($P2_1/n$, No. 14) with lattice parameters $a = 5.394\text{ \AA}$, $b = 14.023\text{ \AA}$, $c = 5.608\text{ \AA}$, and $\beta = 98.50^\circ$ ($Z = 2$) [30]. A prominent feature of lindgrenite structure is the strip of edge-sharing $\text{CuO}_4(\text{OH})_2$ octahedra that runs parallel to the c -axis (Fig. 1). These strips are cross-linked by MoO_4 tetrahedra that share corners with $\text{CuO}_4(\text{OH})_2$ octahedra; each MoO_4 tetrahedron links three strips together, with the fourth linkage occurring along

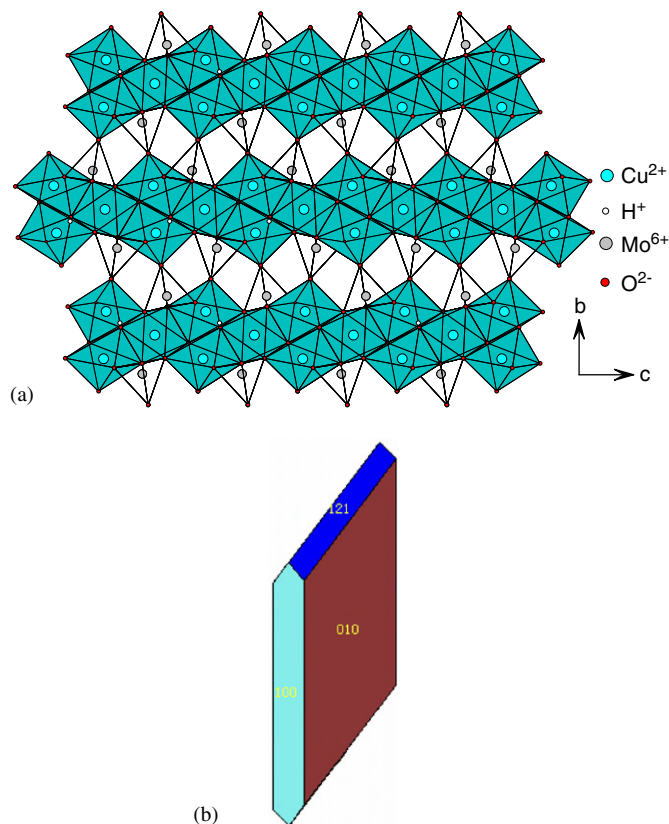


Fig. 1. (a) Strips of edge-sharing $\text{CuO}_4(\text{OH})_2$ octahedra running parallel to the c -axis in lindgrenite crystallographic structure. Transparent tetrahedron represents MoO_4 ; green octahedron represents CuO_6 . (b) Schematic illustration of lindgrenite growth habit, which is obtained from <http://www.webmineral.com/java/Lindgrenite.shtml>. A tubular habit parallel to (010) is predominant, and generally there is an elongation more or less pronounced in the direction of the vertical axis, which is in a good agreement with the previous reports [28].

these strips (Fig. 1). The crystal structure of lindgrenite has some similarities with malachite, which has a layered crystal structure, therefore it can easily form the platelet-like morphology in the absence of any templates [28]. XRD patterns of the as-prepared lindgrenite sample are shown in Fig. 2, and all peaks can be clearly indexed as a pure monoclinic phase of lindgrenite and matched well with the reported data (JCPDS card File No. 86-2311). No diffraction peaks of other phases or amorphous copper compounds were observed in XRD patterns, indicating a high purity and crystallinity of the final products.

Fig. 3 shows the general morphology of the as-prepared lindgrenite samples. The common diameter of the as-prepared lindgrenite microspheres falls in the range of $50\text{--}60\text{ }\mu\text{m}$ with an averaged size of $55\text{ }\mu\text{m}$. Interestingly, the lindgrenite crystallites can self-organize into spherical assemblies or “dandelions” with a puffy appearance. The lindgrenite microspheres are in fact built from small crystal strips that contain even smaller one-dimensional (1D) nanoribbons (as shown in Fig. 1b). These crystal strips, analogous to the “parachutes” in a dandelion, are aligned perpendicularly to the spherical surface, pointing toward a

common center. This one-pot hierarchical organizing scheme relies primarily on geometric constraint of building blocks, which is similar to the previous work [7].

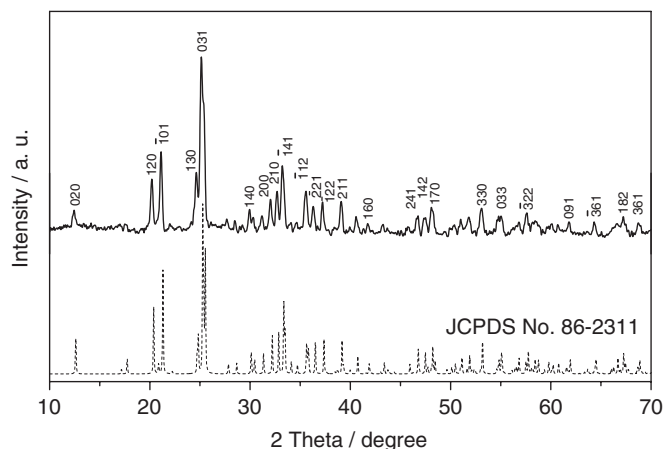


Fig. 2. XRD patterns of hollow and prickly lindgrenite microspheres prepared at 110 °C and 12h. The solid curve is the experimental XRD pattern; the dashed curve is the simulated pattern, which is carried out using the data in JCPDS card File No. 86-2311.

Remarkably, as shown in Fig. 3c, the “dandelions” are coreless with a hollow cavity. The feathery shell comprises loosely packed crystal strips, having communicable inter-crystal space to its central interior. It is observed that the interior surface of these spheres is more compact than the exterior surface (as shown in Figs. 3c and 8b). Under the reported experimental conditions, the lindgrenite products are almost all in this hierarchical morphology.

FT-IR spectra of lindgrenite and $\text{Cu}_3\text{Mo}_2\text{O}_9$ (after the thermal treatment of lindgrenite at 600 °C and 5 h in air, SEM images and XRD pattern are shown in Fig. 9) are shown in Fig. 4. Comparing with the incorporation of OH^- anions in $\text{Cu}_3\text{Mo}_2\text{O}_9$ samples, it is clear that the bands of OH stretching modes in lindgrenite shift to the lower wavenumbers, and split into two bands (as shown in Fig. 4 indicated by the dashed line). This is due to the existence of hydrogen bond in the lindgrenite crystal lattice. The different kinds of bonds in the lindgrenite crystal lattice (which are formed in a different sequence or at different reaction stages) play different roles during the hydrothermal process [21,22]. The hydrogen bonds in the crystal structure (formed at the end of crystallization of lindgrenite, which are different from the Cu–O bonds that

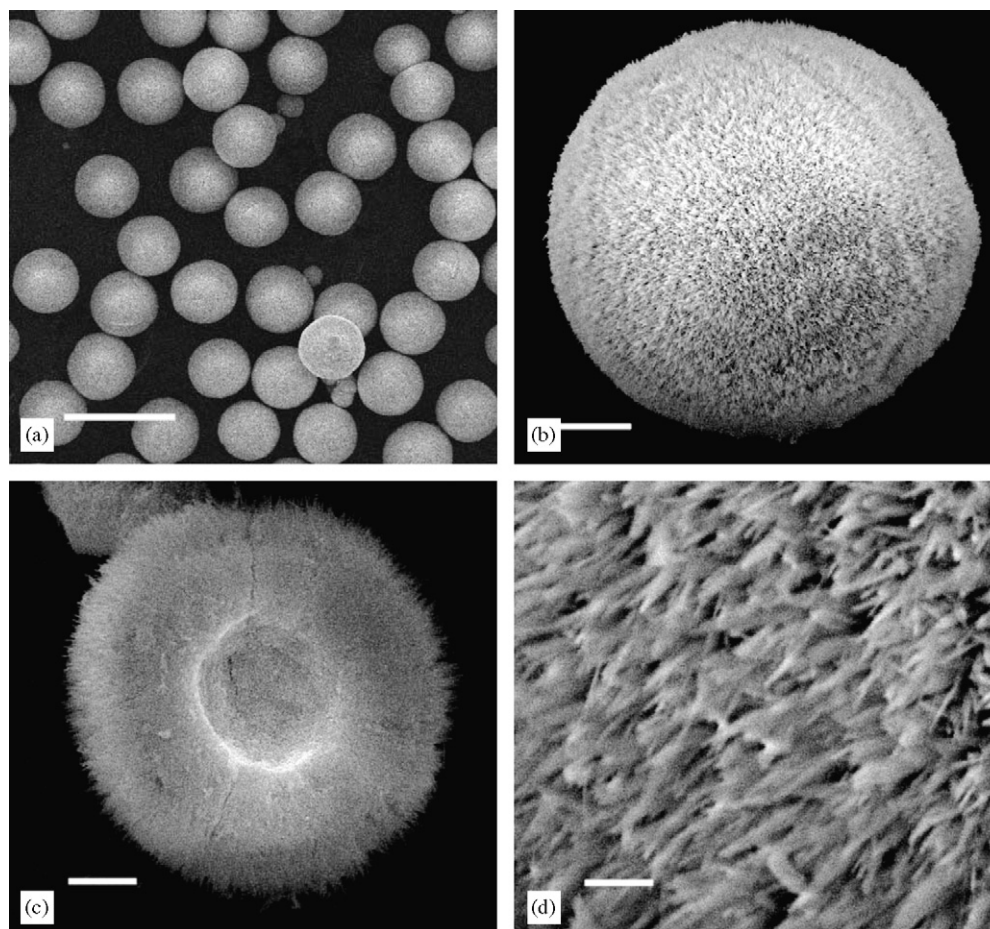


Fig. 3. SEM images of hollow and prickly lindgrenite microspheres prepared at 110 °C and 12h: (a) panoramic morphology, scale bar = 100 μm; (b) a detailed view on an individual sphere, scale bar = 10 μm; (c) the crashed hollow microsphere, scale bar = 5 μm; and (d) the general surface structure of hollow spheres, scale bar = 2 μm.

are formed during the crystallization, and the Mo–O bonds that have been formed before the crystallization of lindgrenite) may have significant effects on the formation

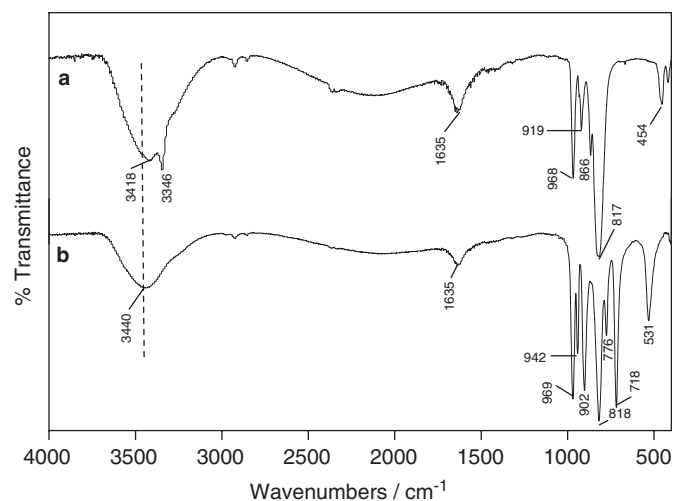


Fig. 4. FT-IR spectra of samples: (a) lindgrenite prepared at 110 °C and 12 h. (b) $\text{Cu}_3\text{Mo}_2\text{O}_9$ obtained from the thermal treatment of the as-prepared lindgrenite at 600 °C and 5 h in air atmosphere.

of rhombic morphology. Some similar experiments have been employed for evaluating the role of hydrogen bonds in crystal growth [26]. It is obvious that peaks appearing in the range of 1300–400 cm^{-1} changed largely after the thermal treatment. This is due to the difference of these two kinds of crystal structures of $\text{Cu}_3(\text{OH})_2(\text{MoO}_4)_2$ and $\text{Cu}_3\text{Mo}_2\text{O}_9$ (mainly due to the difference of Cu–O and Mo–O bands in the crystal lattice). The crystal structure of $\text{Cu}_3(\text{OH})_2(\text{MoO}_4)_2$ consists of strips of edge-sharing CuO_6 octahedra that are cross-linked by MoO_4 tetrahedra [28]. The crystal structure of $\text{Cu}_3\text{Mo}_2\text{O}_9$ consists of strings of corner-sharing CuO_6 octahedra linked to CuO_5 square pyramids and MoO_4 tetrahedra by edges and corners, respectively [17].

Concerning the formation process of hollow and prickly structure, lindgrenite samples prepared at different reaction stages (stage 1 at 50 °C and 1 h; stage 2 at 60 °C and 2 h; stage 3 at 70 °C and 6 h; stage 4 at 80 °C and 8 h) have been, respectively, studied by SEM and XRD measurements. Several obvious evolution stages can be observed and are shown in Figs. 5 and 6. Lindgrenite colloids are initially formed under the synthetic condition, and the initially formed colloids are aggregated together with a spherical

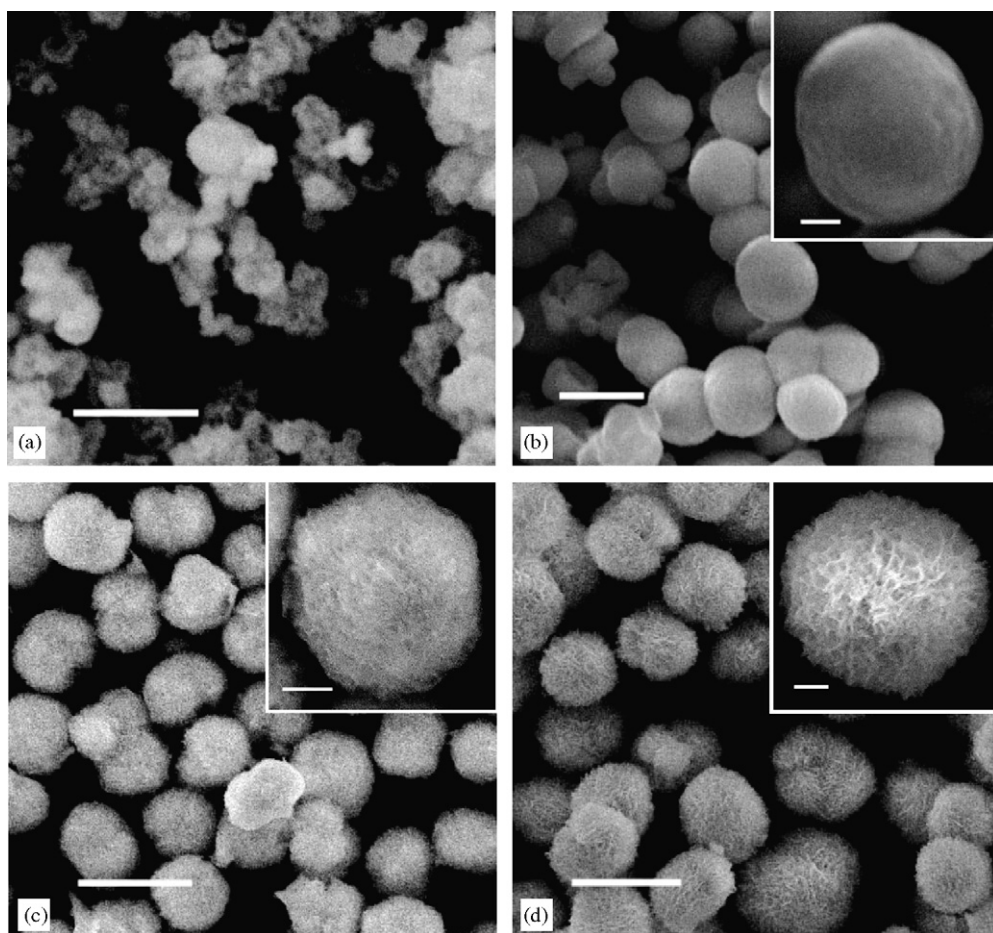


Fig. 5. SEM images of lindgrenite samples prepared at different reaction stages: (a) stage 1 at 50 °C and 1 h, scale bar = 5 μm ; (b) stage 2 at 60 °C and 2 h, scale bar = 5 and 1 μm (inset), respectively; (c) stage 3 at 70 °C and 6 h, scale bar = 10 and 2 μm (inset), respectively; and (d) stage 4 at 80 °C and 8 h, scale bar = 10 and 2 μm (inset), respectively.

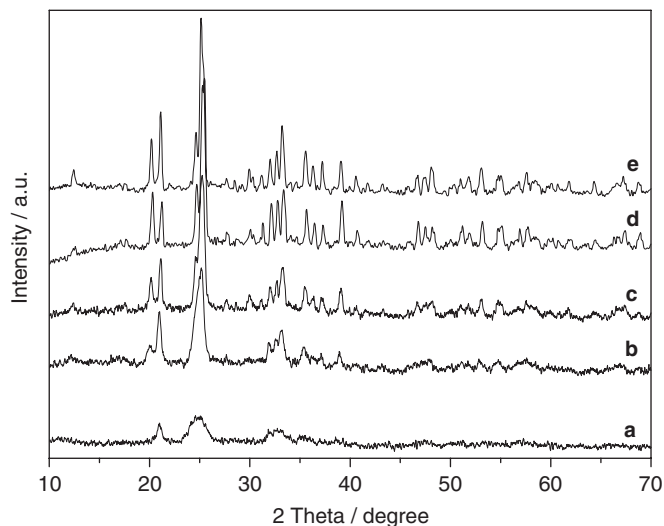


Fig. 6. XRD patterns of lindgrenite samples prepared at different reaction stages: (a) stage 1 at 50 °C and 1 h; (b) stage 2 at 60 °C and 2 h; (c) stage 3 at 70 °C and 6 h; (d) stage 4 at 80 °C and 8 h; and (e) the target sample prepared at 110 °C and 12 h, namely Fig. 2.

appearance, which indicate a nucleation-aggregation mechanism with no room and time for the crystal growth at the high supersaturation level. With the reaction continuing, the concentration of reactants decrease, the reaction rate slows down, the crystal growth rate will gradually become the dominant step, and the prickly lindgrenite crystals appeared on the sphere surface at the end of synthetic process. The formation of lindgrenite hierarchical architecture indicates that the nucleation and growth of lindgrenite are well controlled in our present synthetic process. With the reaction temperature and time increasing, samples have a tendency to gradually crystallize (from XRD patterns of these samples as shown in Fig. 6). Meanwhile, it can be seen that the size of particles of the initial, intermediate, and final stages of samples is gradually enhanced. This result indicates that the whole synthetic system provides an appropriate crystal growth environment for the formation of such a novel hierarchical architecture. Our reaction process might be deduced as a typical Ostwald ripening mechanism, which is perhaps the phenomenon most well known to today's material

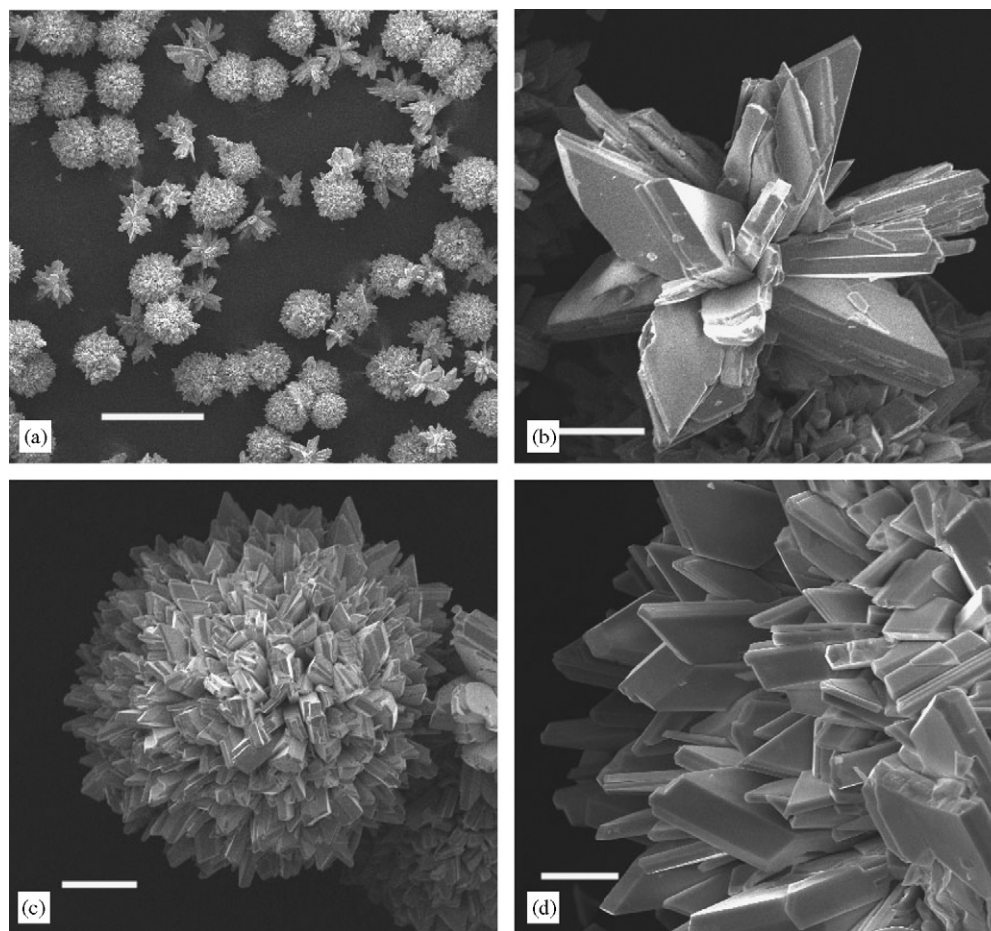


Fig. 7. SEM images of lindgrenite architectures (using CuCl_2 instead of $\text{Cu}(\text{Ac})_2$ as the copper source, prepared at 110 °C and 12 h): (a) panoramic morphology, scale bar = 500 μm ; (b) a detailed view on a flower-like architecture, scale bar = 50 μm ; (c) a detailed view on an individual sphere, scale bar = 50 μm ; and (d) the general surface structure of the as-prepared spheres, scale bar = 20 μm .

chemists. This ripening process involves “the growth of larger crystals from those of smaller size which have a higher solubility than the larger ones” [33,34], and it has been commonly observed in general crystal growth for more than a century.

It is well-known that both intrinsic and extrinsic factors (i.e., the crystal structure and growth environment) have significant effects on the final crystal morphology [35,36]. The geometric shape (habit) of a crystal is determined by the external expression of a selected set of symmetry-related faces. In order to further investigate the formation of the lindgrenite hollow spheres, we have performed a parallel experiment using CuCl_2 instead of $\text{Cu}(\text{Ac})_2$ as the copper source while keeping other reaction conditions the same. Both kinds of similar architectures (including sphere- and flower-like architectures) can be obtained, which are coexistence as shown in Fig. 7. However, the size of these architectures is larger than that in Fig. 3, and the prismatic face can be clearly seen on the surface of these architectures. The main reason is likely to be that the diffuse rate of Cu^{2+} ions in solution is different in both growth environments; the Cu^{2+} ions can easily form complex with CH_3COO^- anions during the formation of lindgrenite architectures [23]. The petal of the flower architecture

clearly shows the growth habit of lindgrenite, which mirrors its crystal nature (comparing Figs. 7b and d with Fig. 1b). The Ostwald ripening process can be well elucidated in the crashed hollow structure as shown in Fig. 8. The smaller crystallites (in the interior surface of spheres) would eventually dissolve into solution and regrow on the larger ones (in the exterior surface of spheres) during Ostwald ripening. This formation process also can be called as a starburst growth, i.e., the lindgrenite crystals grow from the center of sphere, and unfilled voids are left behind and coalesce into large pore. Especially, the lindgrenite crystals have the rhombic growth habit, which is essential for this formation process. And the whole synthetic system provides an appropriate crystal growth environment for the formation of such a novel hierarchical architecture.

According to TGA data of lindgrenite that has been reported in the literature (a broad weight loss in the temperature range 175–400 °C shows the loss of one water molecule to give a final composition of $\text{Cu}_3\text{Mo}_2\text{O}_9$) [32], a simple thermal treatment of the as-prepared sample has been carried out. Interestingly, $\text{Cu}_3\text{Mo}_2\text{O}_9$ with a similar size and morphology can be easily obtained after the thermal treatment in air atmosphere, as shown in Figs. 9

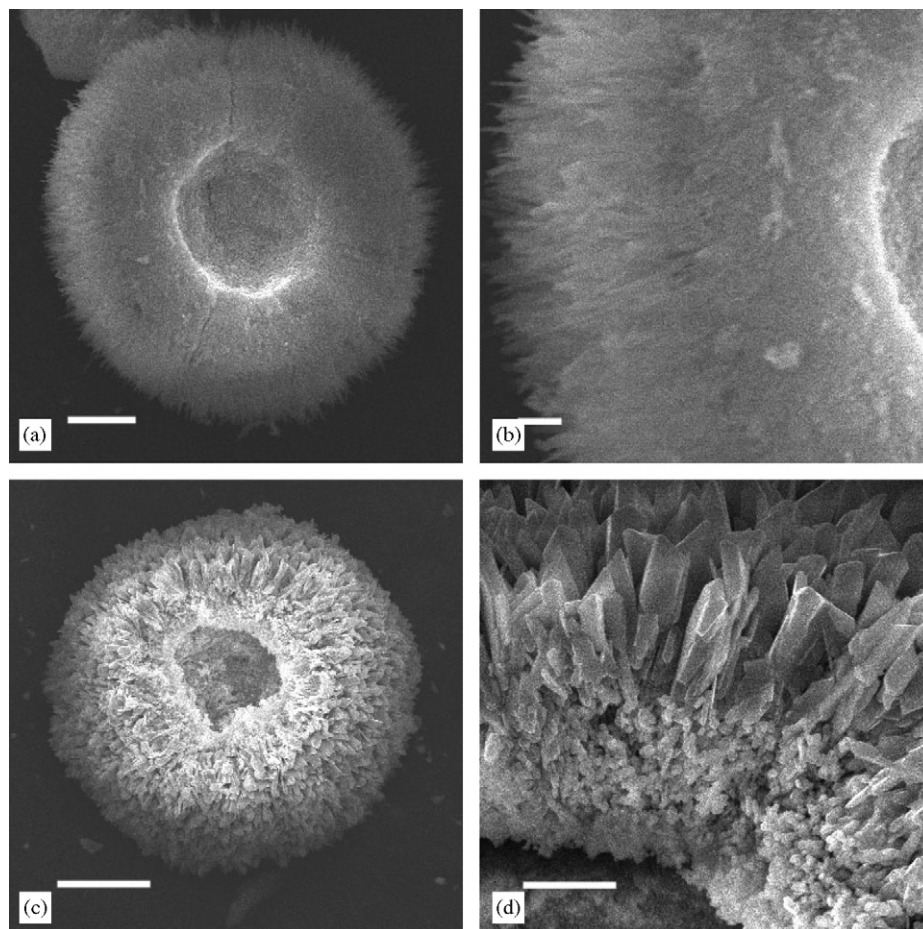


Fig. 8. SEM images of lindgrenite crashed hollow architectures prepared at 110 °C and 12 h: (a) and (b) using $\text{Cu}(\text{Ac})_2$ as the copper source, scale bar = 5 and 1 μm , respectively; (c) and (d) using CuCl_2 as the copper source, scale bar = 20 and 5 μm , respectively.

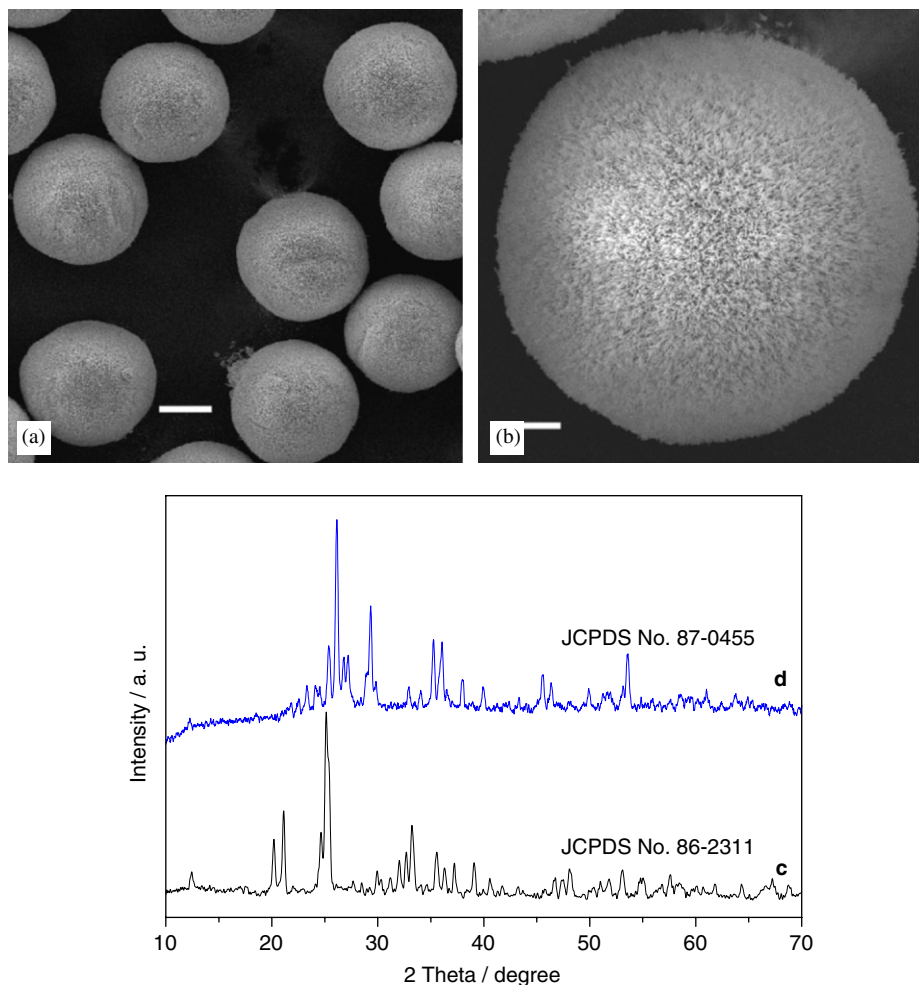


Fig. 9. (a) and (b) SEM images of $\text{Cu}_3\text{Mo}_2\text{O}_9$ obtained from the thermal treatment of the as-prepared lindgrenite at 600°C and 5 h in air atmosphere, scale bar = 50 and 10 μm , respectively. (c) XRD pattern of lindgrenite prepared at 110°C and 12 h (namely Fig. 2). (d) XRD pattern of $\text{Cu}_3\text{Mo}_2\text{O}_9$, obtained from the thermal treatment of the as-prepared lindgrenite at 600°C and 5 h in air atmosphere.

and 4 (thermal treatment conditions: the heating rate is $10^\circ\text{C}/\text{min}$ from room temperature to 600°C , then the temperature is maintained at 600°C for 5 h). The sample color has been changed from green to brown by the thermal treatment of the as-prepared lindgrenite. As one of soot deep oxidation catalysts, $\text{Cu}_3\text{Mo}_2\text{O}_9$ with a high activity has been widely investigated [17,18]. The reports on $\text{Cu}_3\text{Mo}_2\text{O}_9$ morphology are very few, we have demonstrated a novel route to obtain $\text{Cu}_3\text{Mo}_2\text{O}_9$ with such an interesting morphology. The similar processes to obtain target inorganic materials by the direct calcination of their precursors have been successfully applied, which provides a new strategy to prepare inorganic materials with novel morphologies [26].

4. Conclusions

In summary, we have demonstrated a simple and mild hydrothermal approach to fabricate the lindgrenite with a hollow and prickly sphere-like architecture. The possible formation process of such a hierarchical structure has been

elucidated by SEM and XRD measurements, which can be ascribed to a starburst growth process, furthermore, the sphere diameter has a tendency to increase gradually with temperature and time. The traditional Ostwald ripening is an underlying mechanism to form the hollow structure. Another essential factor is the so-called geometric constrains of building blocks (i.e., lindgrenite crystals have a rhombic growth habit), which plays an essential role in the formation of prickly surface. Moreover, $\text{Cu}_3\text{Mo}_2\text{O}_9$ with a similar size and morphology can be easily obtained by a simple thermal treatment of the as-prepared lindgrenite in air atmosphere. This present simple hydrothermal process does not need any inorganic or organic templates, which can easily avoid introducing impurities into the final product, and may also be applicable to the preparation of other inorganic materials.

Acknowledgments

The authors gratefully acknowledge the financial support of the National Natural Science Foundation of China

(NSFC #20471012), a Foundation for the Author of National Excellent Doctoral Dissertation of PR China (FANEDD #200322), the Research Fund for the Doctoral Program of Higher Education (RFDP #20040141004), and the Scientific Research Foundation for the Returned Overseas Chinese Scholars, State Education Ministry.

References

- [1] S. Mann, *Angew. Chem. Int. Ed.* 39 (2000) 3392.
- [2] S. Mann, G.A. Ozin, *Nature* 382 (1996) 313.
- [3] H. Colfen, M. Antonietti, *Angew. Chem. Int. Ed.* 44 (2005) 5576.
- [4] B. Bowden, M. Weck, I.S. Choi, G.M. Whitesides, *Acc. Chem. Res.* 34 (2001) 231.
- [5] F. Caruso, R.A. Caruso, H. Mohwald, *Science* 282 (1998) 1111.
- [6] Y. Sun, Y. Xia, *Science* 298 (2002) 2176.
- [7] B. Liu, H.C. Zeng, *J. Am. Chem. Soc.* 126 (2004) 8124.
- [8] X. Sun, Y. Li, *Angew. Chem. Int. Ed.* 43 (2004) 3827.
- [9] Z. Li, Y. Ding, Y. Xiong, Q. Yang, Y. Xie, *Chem. Commun.* 7 (2005) 918.
- [10] H. Zhu, X. Ji, D. Yang, Y. Ji, H. Zhang, *Microporous Mesoporous Mater.* 80 (2005) 153.
- [11] Z. Yang, W. Zhang, Q. Wang, X. Song, Y. Qian, *Chem. Phys. Lett.* 418 (2006) 46.
- [12] A.K. Cheetham, *Science* 264 (1994) 794.
- [13] A. Moini, R. Peascoe, P.R. Rudolf, A. Clearfield, *Inorg. Chem.* 25 (1986) 3782.
- [14] X. Cui, S. Yu, L. Li, L. Biao, H. Li, M. Mo, X. Liu, *Chem. Eur. J.* 10 (2004) 218.
- [15] H. Shi, L. Qi, J. Ma, N. Wu, *Adv. Funct. Mater.* 15 (2005) 442.
- [16] Y. Cheng, Y. Wang, D. Chen, F. Bao, *J. Phys. Chem. B* 109 (2005) 794.
- [17] U. Steiner, W. Reichelt, *Acta Crystallogr. C* 53 (1997) 1371.
- [18] M. Hasan, M. Zaki, K. Kumari, L. Pasupulety, *Themochim. Acta* 320 (1998) 23.
- [19] C. Canevali, F. Morazzoni, R. Scotti, D. Cauzzi, P. Moggic, G. Predieri, *J. Mater. Chem.* 9 (1999) 507.
- [20] S.S. Kim, S. Ogura, H. Ikuta, Y. Uchimoto, M. Wakihara, *Solid State Ion.* 146 (2002) 249.
- [21] J. Xu, D. Xue, *J. Phys. Chem. B* 110 (2006) 17400.
- [22] J. Xu, D. Xue, *J. Phys. Chem. B* 110 (2006) 11232.
- [23] R. Rodriguez-Clemente, C.J. Serna, M. Ocana, E.J. Matijevic, *J. Cryst. Growth* 143 (1994) 277.
- [24] H.C. Lichenegger, T. Schoberl, M.H. Bartl, H. Waite, G.D. Stucky, *Science* 298 (2002) 389.
- [25] J. Xu, D. Xue, *J. Phys. Chem. B* 110 (2006) 7750.
- [26] J. Xu, D. Xue, *J. Phys. Chem. B* 109 (2005) 17157.
- [27] F. Xiao, J. Sun, X. Meng, R. Yu, H. Yuan, D. Jiang, S. Qiu, R. Xu, *Appl. Catal. A-Gen.* 207 (2001) 267.
- [28] C. Palache, *Am. Mineral.* 20 (1935) 484.
- [29] L.D. Calvert, W.H. Barnes, *Can. Mineral.* 6 (1957) 31.
- [30] F.C. Hawthorne, R.K. Eby, *Neues Jb. Miner. Monats.* 5 (1985) 234.
- [31] R.L. Frost, L. Duong, M. Weler, *Neues Jb. Miner. Abh.* 180 (2004) 245.
- [32] K. Pavani, A. Ramanan, *Eur. J. Inorg. Chem.* (2005) 3080.
- [33] P. Ball, M. Ruben, *Angew. Chem. Int. Ed.* 43 (2004) 4842.
- [34] W.Z. Ostwald, *Phys. Chem.* 22 (1897) 289.
- [35] D. Xu, D. Xue, *J. Cryst. Growth* 286 (2006) 108.
- [36] J. Xu, D. Xue, *J. Phys. Chem. Solids* 67 (2006) 1427.